Title

Off-resonance saturation ratio obtained with ultrashort echo time-magnetization transfer techniques is sensitive to changes in static tensile loading of tendons and degeneration

Journal

Journal of Magnetic Resonance Imaging, 42(4)

ISSN

1053-1807

Authors

Chang, Eric Y
Du, Jiang
Biswas, Reni
et al.

Publication Date

2015-10-01

DOI

10.1002/jmri.24881

Off-Resonance Saturation Ratio Obtained With Ultrashort Echo Time-Magnetization Transfer Techniques Is Sensitive to Changes in Static Tensile Loading of Tendons and Degeneration

Eric Y. Chang, MD,[1,2] Jiang Du, PhD,[2] Reni Biswas, BS,[2] Sheronda Statum, MS,[2] Chantal Pauli, MD,[3] Won C. Bae, PhD,[2] and Christine B. Chung, MD[1,2]

Background: To determine if off-saturation ratio (OSR) measured with the ultrashort echo time magnetization transfer (UTE-MT) sequence could differentiate between tendons under different states of tensile load and to compare these changes between normal versus degenerated tendons.
Methods: Fourteen tendons were imaged at 3 Tesla before and during the application of 0.5–1 kg tension. A two-dimensional (2D) -UTE-MT sequence with 1.5, 3, and 5 kHz frequency offsets was used on nine tendons and a 3D-UTE-MT sequence with 1.5 kHz frequency offset was used on five tendons. OSR was calculated and compared for each condition. Histologic correlation was performed using light microscopy.
Results: In general, OSR increased after the application of tension. Mean increase of 2D OSR was 0.035 (95% confidence interval [CI], 0.013–0.056) at 1.5 kHz offset ($P < 0.01$), 0.031 (95% CI, 0.023–0.040) at 3 kHz offset ($P < 0.01$), and 0.013 (95% CI, −0.013–0.027) at 5 kHz offset ($P = 0.07$) from pre- to posttension states. Mean increase of 3D OSR was 0.026 (95% CI, 0.008–0.044) at a 1.5 kHz offset ($P = 0.02$) from pre- to posttension states. Mean decrease of 2D OSR at 1.5 kHz offset was 0.074–0.087 when comparing normal versus degenerated tendons ($P < 0.01$).
Conclusion: OSR as measured with 2D or 3D UTE-MT sequences can detect the changes in hydration seen when tendons are placed under two different states of tensile load, but these changes are smaller than those encountered when comparing between normal versus pathologic tendons. Lower off-resonance saturation frequencies (3 kHz or less) are more sensitive to these changes than higher off-resonance saturation frequencies.

J. MAGN. RESON. IMAGING 2015;42:1064–1071.

TENDONS ARE INTEGRAL for joint motion, generally serving to connect muscle to bone.[1] Tendon dysfunction and injuries produce considerable morbidity for those afflicted. Unfortunately, diagnosis and management of subtle alteration in tendon structure pose a considerable challenge for clinicians.[2]

Human tendon composition varies by location and disease state, but healthy tendon is approximately 66–75% water and the dry weight is approximately 65–87% type I collagen, although other collagen types and proteoglycans are also present.[3,4] The unique composition and highly ordered structure of tendons leads to rapid transverse relaxation and limited opportunity for signal encoding with conventional MR imaging techniques.[5] Ultrashort echo time (UTE) sequences have been used to detect signal in tendon as well as differentiate between normal and pathologic tendons.[6,7]

More recently, UTE sequences have been combined with magnetization transfer (MT) techniques for the assessment of tissues with rapid mean transverse decay, including tendons.[8–11] Specifically, the application of an off-resonance radiofrequency saturation pulse modifies the standard UTE MRI sequence and sensitizes the signal to proton pools with extremely fast transverse relaxation (i.e., water bound to collagen) [12] that are not otherwise detectable on clinical

View this article online at wileyonlinelibrary.com. DOI: 10.1002/jmri.24881

Received Oct 22, 2014, Accepted for publication Feb 18, 2015.

*Address reprint requests to: E.Y.C., VA San Diego Healthcare System, San Diego, CA 92161. E-mail: ericchangmd@gmail.com

From the [1]Radiology Service, VA San Diego Healthcare System, San Diego, California, USA; [2]Department of Radiology, University of California, San Diego Medical Center, San Diego, California, USA; and [3]Institute of Surgical Pathology, University Hospital Zurich, Zurich, Switzerland.

scanners.[13] The 3D-UTE techniques with MT preparation show strong translational potential because of shorter imaging times compared with relaxometry techniques, with groups successfully using protocols as short as 3–4 min.[11,14]

The off-resonance saturation ratio (OSR) is a quantitative measure obtained from UTE-MT sequences that can be assessed, reflecting both direct saturation and true MT effects.[8,10,11] Using a 3D-UTE sequence in combination with an off-resonance saturation pulse, Grosse et al found that OSR values were significantly lower in symptomatic patients with tendinopathy compared with healthy volunteers.[11] The same group also found that OSR values were sensitive to short-term exercise-induced changes, with increasing values after high intensity rope skipping and cross-country running.[8]

While OSR may be sensitive to changes in tendons due to high-intensity exercise, to our knowledge, the effect of smaller, tensile loads on OSR has not been studied. Knowledge of these effects would be useful when comparing values between ex vivo specimens and the in vivo condition where muscle tone exists, or when studying tendons in the setting of pathological muscle tone. The purpose of this study was to determine if OSR as measured with the UTE-MT sequence could be used to differentiate between tendons that were subjected to different states of static tensile load and to compare these changes between normal versus degenerated tendons.

Materials and Methods

Sample Preparation

This anonymized cadaveric study was exempted from formal review by the Institutional Review Board. For this project, 15 tendon samples were harvested from three donor ankles (two females, one male; mean age 87 years old). Tendons included the tibialis anterior, tibialis posterior, flexor digitorum longus, flexor hallicus longus, extensor hallicus longus, and peroneus longus tendons. Specimens had undergone a single freeze–thaw cycle before dissection. Tendon samples were cut to 4–6 cm in length and a Krackow stitch [15] was tied over 1 cm to each end, allowing both the core and periphery of the tendon to be tensioned simultaneously. Tendons were immersed into normal saline for 12 h at 4°C, gently blotted dry, and individually placed into separate sealed plastic syringes filled with Fomblin to minimize dehydration and susceptibility artifact.[16] Sutures were fixed to one end of the syringe by a red Luer Lock cap and long suture tails were extended from the opposite plunger end which contained a rubber stopper seal, similar to what was performed in a previous experiment.[17] Tendons were imaged parallel to the long axis of the magnet bore. At the time of imaging, tendon specimens had been at room temperature for at least 4 h.

Tensile Loading and MR Imaging Protocol

Imaging was performed on a 3 Tesla (T) clinical MRI scanner (Signa Twinspeed, GE Healthcare, Milwaukee, WI). Hardware modification included an addition of a custom transmit–receive switch to the receiver preamplifiers for rapid switching after the end of a radiofrequency excitation pulse, which allowed for early detection of signal for UTE imaging. Tendons were imaged with a wrist coil (BC-10, Medspira, Minneapolis, MN). One suture end of each tendon was tied to the table and the other suture end was extended out of the magnet bore.

Ten tendons were imaged while lax (no tensile load applied) and again after a 1-liter water bottle (weighing 1 kilogram each) was tied to the mobile suture end of each tendon at the edge of the table. During the loading phase, sutures for one tendon specimen failed and this sample was excluded from this study. Tensile load was applied for at least 90 minutes before the start of imaging under load to allow for equilibrium of viscoelastic creep.[18,19] For these nine tendons, a two-dimensional (2D) -UTE-MT imaging protocol was used which included: repetition time (TR) = 400 ms, echo time (TE) = 8 μs, field of view (FOV) = 10 cm, slice thickness = 1.7 mm, matrix = 512 × 512, without and with MT pulse preparation, which consisted of a Fermi pulse of 8 ms duration, pulse power 1200, and frequency offsets of 1.5, 3, and 5 kHz. Frequency offsets were chosen based on previously published studies using Achilles tendons [11,14] and MT pulse duration and power were chosen to fall within specific absorption rate (SAR) limits. Total imaging time for the entire 2D-UTE-MT protocol was approximately 30 min. A rubber eraser was placed in the field of view of each 2D scan as an external control. To ensure comparable image locations between pre- and posttension scans, tendons were imaged in the axial plane at the approximate midportion of each tendon in the longitudinal axis. The approximate midportion was determined using low-resolution localizer images.

Five tendons were imaged with the tendons lax (no tensile load applied) and again after a 0.5-liter water bottle (weighing 0.5 kilograms each) was tied to the mobile suture end of each tendon at the edge of the table. Again, tensile load was applied for at least 90 min before the start of imaging under load to allow for equilibrium of viscoelastic creep. For these five tendons, a 3D-UTE-MT imaging protocol was used which included: TR = 50 ms, TE = 30 μs, FOV = 8 cm, slice thickness = 0.3 mm, matrix = 256 × 256 × 256, without and with MT pulse preparation, which consisted of a Fermi pulse of 8 ms duration, pulse power 540°, and frequency offset of 1.5 kHz. Frequency offset was chosen based on a previously published study showing that frequencies < 3 kHz showed slightly higher differences between healthy and diseased tendons compared with those > 3 kHz.[11] MT pulse duration and power were chosen to fall within specific absorption rate (SAR) limits. Total imaging time for the entire 3D-UTE-MT protocol was approximately 38 min.

Image Analysis

Using axial images at the midportion of each tendon in the longitudinal axis, regions of interest (ROIs) were carefully placed by a single fellowship-trained musculoskeletal radiologist (4 years of experience with quantitative imaging) within the boundaries of the epitenon on the image without saturation pulse and digitally copied to the UTE-MT images with various offset saturation frequencies. The off-resonance saturation ratio (OSR) at each frequency for each sequence was calculated: $OSR = \frac{S_0 - S_{SAT}}{S_0}$, where S_0 denotes the mean signal intensity acquired without a saturation pulse and S_{SAT} denotes the mean signal intensity acquired with the saturation

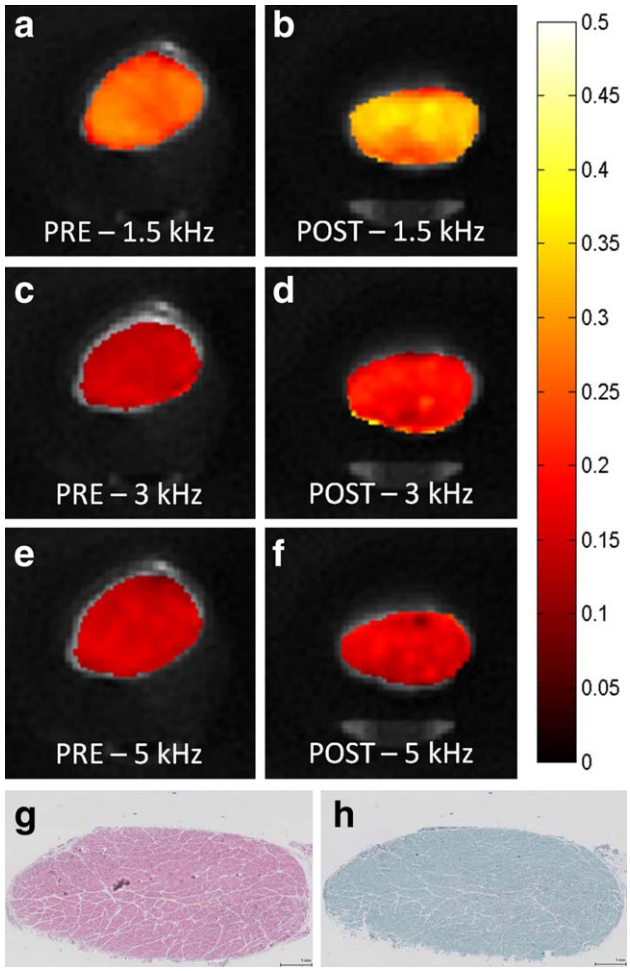

FIGURE 1: The 2D-UTE-MT images of a normal tibialis anterior tendon with overlaid OSR pixel maps before (A,C,E) and after (B,D,F) 1 kg tension, using 1.5 kHz (A,B), 3 kHz (C,D), and 5 kHz (E,F) off-resonance saturation pulses with corresponding histologic slides (G,H). Global ROI at 1.5 kHz measured 0.26 pretension (A) and increased to 0.32 posttension (B). Global ROI at 3 kHz measured 0.15 pretension (C) and increased to 0.19 posttension (D). Global ROI at 5 kHz measured 0.15 pretension (E) and increased to 0.17 posttension (F). No degeneration was noted on H&E (G) and Saf-O (H) stains (original magnification 40×) for this specimen.

pulse. Global ROI OSR was calculated as well as pixel maps, using a semiautomated MATLAB (The Mathworks Inc., Natick, MA) code.

For the nine tendons imaged with the rubber eraser control, the total water content for each tendon was calculated on the 2D-UTE images. The rubber eraser was used as a control to account for differences in transmit-receive gain and image rescaling. The normalized signal intensity of the tendon (S_{norm}) was calculated as: $S_{norm} = \frac{S_{ten}}{S_{eras}}$, where S_{ten} denotes the mean signal intensity of the tendon, and S_{eras} denotes the mean signal intensity of the eraser. S_{norm} before and after loading is expected to provide information on changes in water concentration due to loading.

Histologic Analysis

After MR imaging, tendons were carefully sectioned in the same axial plane as the images. Specifically, the midportion of each tendon in the longitudinal axis was used to ensure comparable regions. Each tendon piece was fixed in 10% zinc formalin, dehydrated with alcohol, and embedded in paraffin. Sections were cut and stained with hematoxylin and eosin (H&E) and Safranin-O-Fast Green (Saf-O) to evaluate for collagen structural integrity and proteoglycan content, respectively.[20] Tendons were evaluated for signs of tendinosis, including abnormal tenocyte morphology, increased vascularity, presence of calcification, chondroid metaplasia, fatty/mucoid degeneration, or proteoglycan/GAG deposition.[21,22] A pathologist examined all sections (C.P., 8 years of experience in musculoskeletal histopathology) and was blinded to the MRI results.

Statistical Analysis

Statistical analyses were performed using the SPSS software package (version 21; SPSS, Chicago, IL). The Shapiro-Wilk test for normality was performed on the data. Descriptive statistics were reported for each condition and imaging sequence, and included the mean for normally distributed data and the median for nonparametric data. Bland-Altman plots were created for the pretension and posttension conditions. Comparisons between the pretension and posttension conditions were performed, including paired-samples t-tests for normally distributed data and Wilcoxon Signed Ranks tests for nonparametric data. Comparison between OSR of degenerated versus normal tendons were performed. Statistical significance was defined as a *P*-value less than 0.05.

Results

Both the 2D-UTE-MT and 3D-UTE-MT sequences provided images which could be used to generate OSR maps of the nine and five ankle tendons, respectively (Figs. 1–3). Quantitative results for the global ROIs are summarized in Tables 1 and 2.

In general, OSR increased after the application of tension (Figs. 4–6), with statistically significant differences between the pretension and posttension conditions found using the 2D-UTE-MT sequence with 1.5 and 3 kHz frequency offset saturation pulses ($P = 0.006$ and $P < 0.001$, respectively) as well as the 3D-UTE-MT sequence with a 1.5 kHz frequency offset saturation pulse ($P = 0.017$). Statistical significance was not reached when comparing between the pretension and posttension conditions using the 2D-UTE-MT sequence and a 5 kHz frequency offset saturation pulse ($P = 0.07$). In only two instances did OSR decrease after tension, and both cases involved flexor digitorum longus tendons (from different donors), and were the two smallest tendons by cross-sectional area in our study. For the nine tendons, there was no significant difference detected between the normalized signal intensity for the pretension condition (median, 1.76; 95% confidence interval [CI], 1.70–1.82; range, 1.69–2.04) versus the posttension condition (median, 1.75; 95% CI, 1.60–1.84; range, 1.23–1.89) ($P = 0.123$).

Of the nine tendons that underwent 2D-UTE-MT imaging, three demonstrated histologic signs of mild degeneration

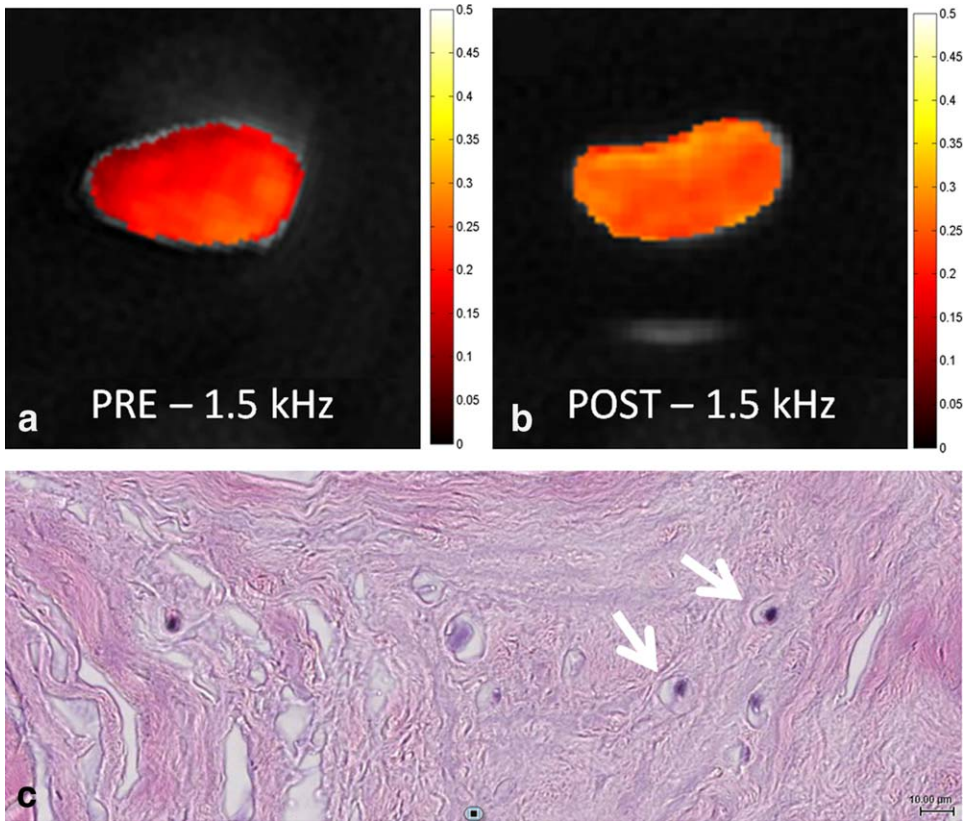

FIGURE 2: The 2D-UTE-MT images of a degenerated posterior tibialis tendon with overlaid OSR pixel maps before (A) and after (B) 1 kg tension, using 1.5 kHz off-resonance saturation pulse with corresponding histologic slide (C). Global ROI at 1.5 kHz measured 0.20 pretension (A) and increased to 0.24 posttension (B). On H&E slide with 40x magnification (C), mild mucoid degeneration with chondroid metaplasia is present (arrows), consistent with tendinosis.

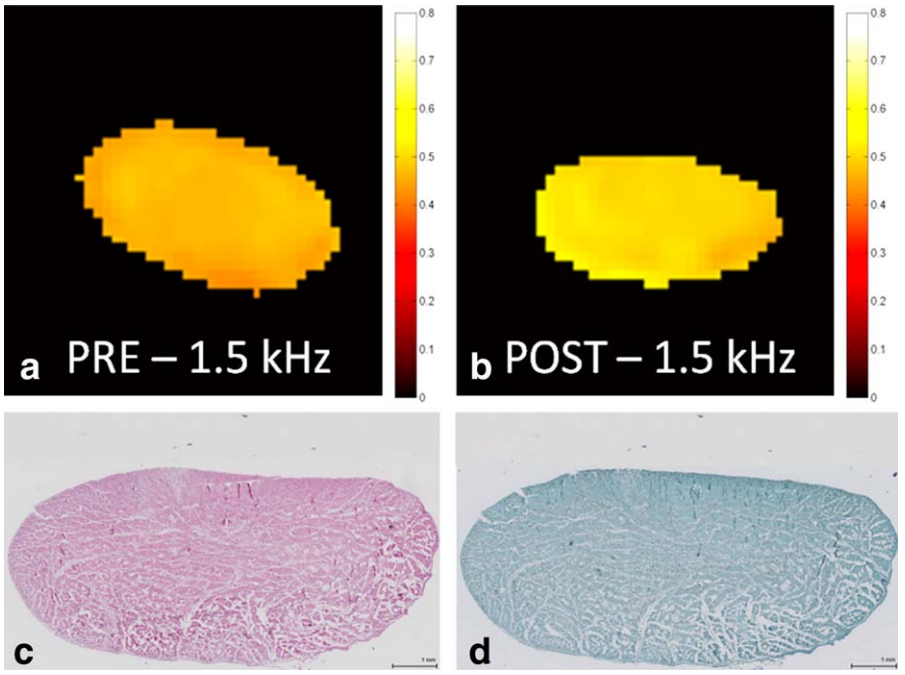

FIGURE 3: Tibialis posterior tendon imaged with 3D-UTE-MT sequence with OSR pixel maps before (A) and after (B) 0.5 kg of tension and corresponding histologic slides (C,D). Global ROI measured 0.52 pretension (A) and increased to 0.55 posttension (B). Although artificial separation of tendon fascicles was noted at the inferior aspects of the H&E (C) and Saf-O (D) stains (original magnification 40×), consistent with tissue freezing and thawing, no degeneration was noted for this specimen.

TABLE 1. 2D-UTE-MT OSR Results (Nine Samples)

Frequency offset (kHz)	Mean pre-tension OSR [range]	Mean post-tension OSR [range]	Mean difference	95% CI of the difference	*P*-value[a]
1.5	0.270 [0.192-0.339]	0.305 [0.241-0.384]	−0.035	−0.056 – −0.013	0.006
3	0.150 [0.126-0.172]	0.182 [0.154-0.212]	−0.031	−0.040 – −0.023	0.000
5	0.155 [0.131-0.175]	0.168 [0.139-0.221]	−0.013	−0.027 – 0.013	0.070

[a]Calculated by paired samples t-tests.

TABLE 2. 3D-UTE-MT OSR Results (Five Samples)

Frequency offset (kHz)	Mean pre-tension OSR [range]	Mean post-tension OSR [range]	Mean difference	95% CI of the difference	*P*-value[a]
1.5	0.478 [0.448-0.514]	0.504 [0.460-0.547]	−0.026	−0.044 – −0.008	0.017

[a]Calculated by paired samples t-tests.

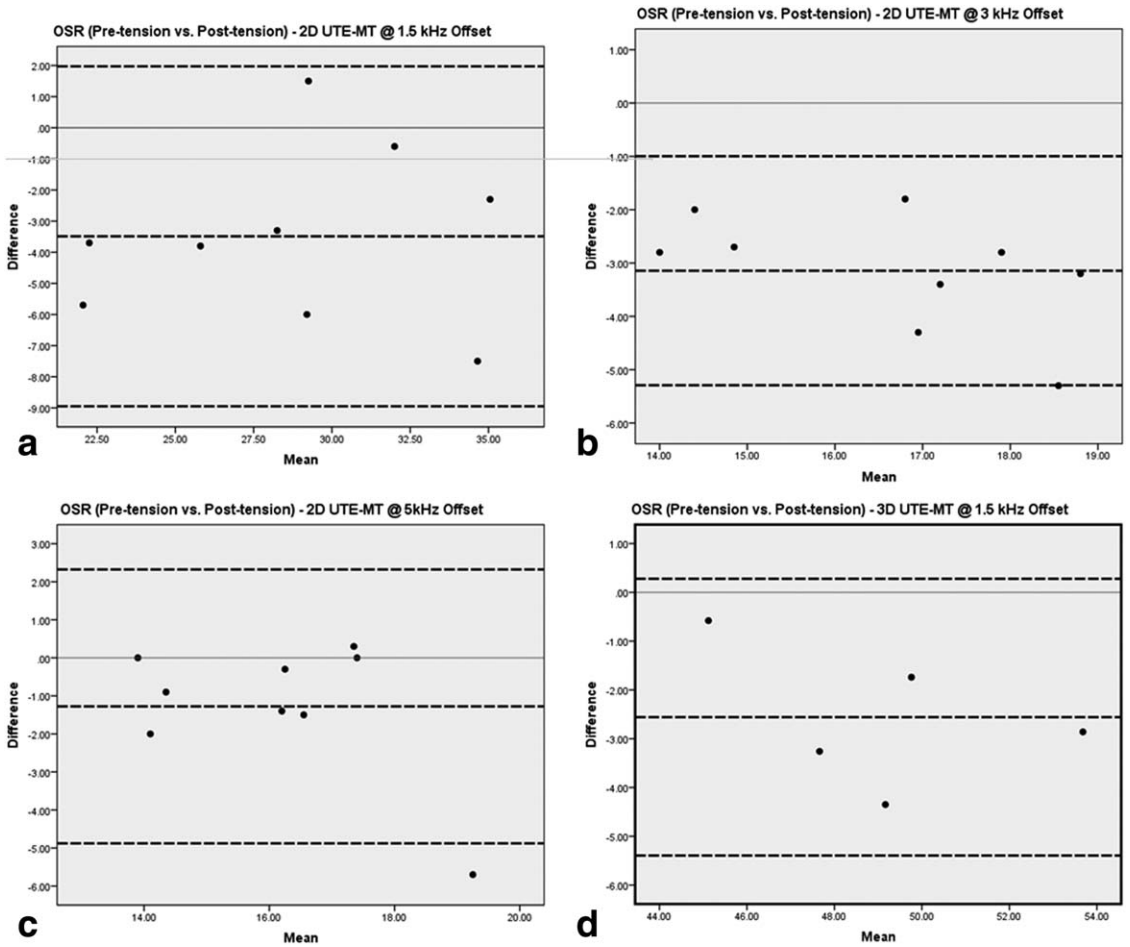

FIGURE 4: Bland-Altman plots illustrating the difference between pretension and posttension conditions. In general, OSR increased after the application of tension for nearly all specimens with systematic bias of −3.49 using 2D UTE-MT at 1.5 kHz offset (A), −3.14 using 2D-UTE MT at 3 kHz offset (B), −1.28 using 2D-UTE MT at 5 kHz offset (C), and −2.56 using 3D-UTE MT at 1.5 kHz offset (D).

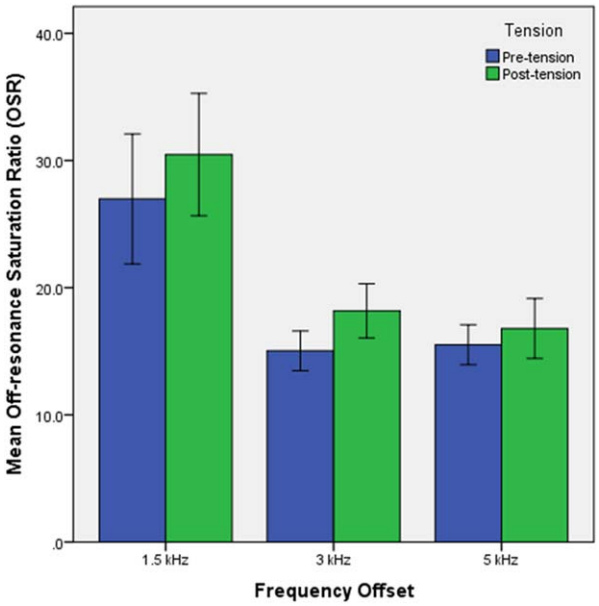

FIGURE 5: Mean off-resonance saturation ratios obtained with 2D-UTE-MT sequence for nine tendons using 1.5, 3, and 5 kHz off-resonance saturation pulses before and after 1 kg of tension. The error bars indicate standard deviation of the group mean.

and 6 were classified as normal. All five tendons that underwent 3D-UTE-MT imaging were histologically normal. Mean OSR was higher for the normal samples (n = 6) (Fig. 1) compared with the degenerated samples (n = 3) (Fig. 2) for all frequency offsets and tension states, although only the 1.5 kHz frequency offset reached significance (Table 3).

Discussion

In this study, we imaged tendons before and after the application of 1 kg and 0.5 kg of tension using 2D and 3D UTE-MT sequences, respectively, and found that OSR was significantly different between lax tendons and tendons under small amounts of tension (0.5–1 kg). Previous studies have demonstrated that tensile loading of tendons leads to a decrease in total water content [23,24] and our results suggest that OSR is able to detect these subtle alterations in water status. These findings can be contrasted with a recent study from our lab, where there was no significant difference between T2* values of lax tendons and tendons under 1 kg of tension.[17] Taken together, these results suggest that OSR is more sensitive to subtle alterations with tension compared with T2*.

It is well known that MT measurements vary depending on tissue and are highly dependent on the particular experimental procedures used, including field strength as well as the off-resonance frequency and power of the saturation pulse.[25] However, our results can be compared with those from Grosse et al [11] who also used a 3D-UTE sequence at 3T in combination with a 1.5 kHz off-resonance saturation pulse. In their study on Achilles tendons, the authors found a mean OSR value of 0.38 for healthy tendons and 0.27–0.30 for tendinopathic tendons.[11] We confirm their findings that healthy tendons demonstrate higher OSR values compared with degenerated tendons. Using similar parameters, our mean values obtained on the smaller tendons in the lower extremity yielded higher overall OSR values with means ranging from 0.48 pretension to 0.50 posttension. This likely reflects differences in composition, structure and function between the Achilles tendon and other tendons of the lower extremity which were used for this study.[26] Of note, the mean difference between pre- and posttension states in our sample was 0.03, whereas the mean difference found between normal and pathologic tendons was 0.07–0.09 at 1.5 kHz offset frequency (comparable to 0.08–0.11 reported by Grosse et al).[11] Our results suggest that caution should be used when directly comparing OSR values between cadaveric tissue (without muscle tone) and values obtained in vivo (with resting muscle tone) for both 2D and 3D UTE-MT sequences at 1.5 kHz and 3 kHz; however, the magnitude of change between normal and pathologic tissue is greater.

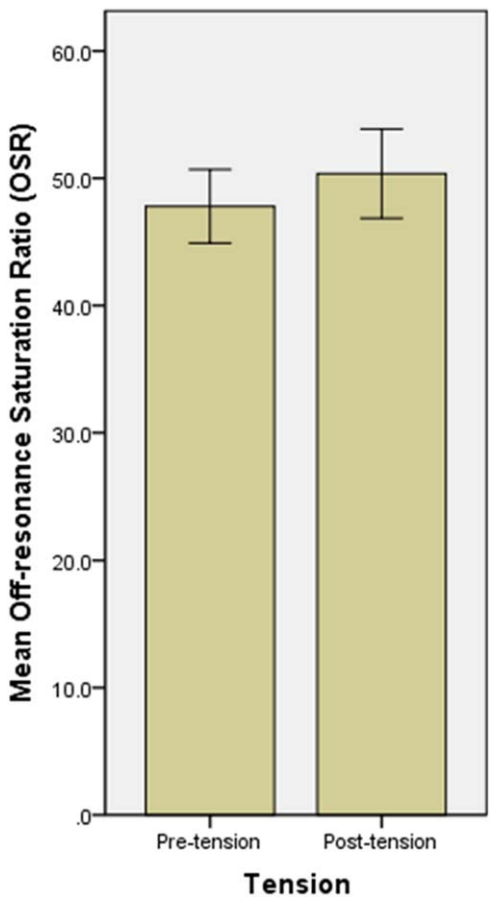

FIGURE 6: Mean off-resonance saturation ratios obtained with 3D-UTE-MT sequence and 1.5 kHz off-resonance saturation pulse for five tendons before and after 0.5 kg of tension. The error bars indicate standard deviation of the group mean.

TABLE 3. Results for Normal (n=6) versus Degenerated (n=3) Samples Using 2D-UTE-MT

Frequency Offset (kHz), Tension State	Normal Samples: Mean OSR [range]	Degenerated Samples: Mean OSR [range]	Mean Difference	95% CI of the Difference	*P*-value[a]
1.5 kHz, pre-tension	0.299 [0.262-0.339]	0.212 [0.192-0.239]	0.087	[0.040 – 0.135]	0.003
1.5 kHz, post-tension	0.329 [0.285-0.384]	0.256 [0.241-0.277]	0.074	[0.018 – 0.129]	0.005
3 kHz, pre-tension	0.156 [0.135-0.172]	0.138 [0.126-0.155]	0.018	[-0.005 – 0.041]	0.105
3 kHz, post-tension	0.190 [0.162-0.212]	0.166 [0.154-0.189]	0.024	[-0.007 – 0.056]	0.111
5 kHz, pre-tension	0.161 [0.139-0.175]	0.143 [0.131-0.158]	0.019	[-0.004 – 0.041]	0.092
5 kHz, post-tension	0.175 [0.148-0.221]	0.154 [0.139-0.173]	0.020	[-0.018 – 0.058]	0.246

[a]Calculated by independent samples t-tests.

With off-resonance saturation frequencies less than 3 kHz, direct saturation effects dominate the signal decrease seen with the UTE-MT sequence, whereas with frequencies greater than 3 kHz, true magnetization transfer effects dominate the signal decrease.[14] In the present study, OSR values with lower frequency offsets (dominated by direct saturation effects) showed greater mean differences between the two tension conditions. These results are also similar to the study by Grosse et al where off-resonance values less than 3 kHz showed slightly higher differences between healthy and affected tendons compared with values greater than 3 kHz.[11]

In our study, we were unable to detect a significant difference when comparing normalized signal intensity before and after the application of 1 kg of weight. In contrast, Helmer et al found that changes in tendon hydration could be detected using a one-dimensional proton-density map on Achilles tendons of New Zealand white rabbits after the application of 7.5N (0.76 kg).[18] Because it is known that tendons decrease in water content after tension, the discrepancy may be explained by the differences in tendon caliber between the two studies. New Zealand White rabbit Achilles tendons are much smaller in cross-sectional area compared with human lower extremity tendons used in this study.[27,28] This would lead to higher degrees of strain and yield greater changes in hydration that may be easier to detect.

Our study has several limitations. First, a small number of samples were used. Our study had adequate power to detect a significant difference in OSR between the two tension states for both 2D (1.5 and 3 kHz frequency offsets) and 3D-UTE-MT (1.5 kHz frequency offset) sequences. However, differences in means for the 2D-UTE-MT sequence at 5 kHz offset did not reach significance, likely due to low power. The results from this pilot study require external validation with larger sample sizes and tendons from other locations. Second, our histologic technique consisted only of conventional light microscopy. However, it is known that electron microscopy is more sensitive for degenerative tendinopathy.[29] Third, we applied a fixed load and thus did not standardize the strain between the tendons of different sizes. Tendons subject to different strains will likely yield differences in calculated OSR. In two outlier cases, OSR decreased after tension, both involving flexor digitorum longus tendons. Although the reason remains unclear, the fact that these outliers involved the smallest tendons in our pilot study deserves additional study in future experiments using different sample sizes and loads.

Additionally, different tensile loads were used for the 2D and 3D sequences. However, 4-0 sutures were used for extension to connect the water bottle and the 1 kg weight exceeded the suture tensile capacity for one specimen. Thereafter a 0.5 kg was used for the 2D sequences which fell within the tensile strength limits for 4-0 nylon suture. Future studies may benefit from using newer generation polyethylene sutures, which may have improved biomechanical properties. Furthermore, without the use of isotropic 3D sequences on all specimens, the amount of tendon elongation and strain could not be measured. Fourth, comparing identical regions in deforming tissue is quite challenging, particularly with 2D imaging. To ensure comparability, we used the midportion because sutures were tied over equal lengths to both ends. This was determined using localizer images and there may have been slight errors in approximation. Fifth, we did not measure the total amount of water loss between the two tension states, which requires accurate and lengthy measurements of T1 and T2* of the tendons and rubber eraser, as well as proton density of the rubber eraser. Finally, we did not measure OSR and water content changes in tendons with multiple loading states. It is likely that more significant changes in OSR and water content will be observed with increased loading.

In conclusion, we have shown in our pilot study that OSR as measured with 2D or 3D UTE-MT sequences can

detect the small changes in hydration seen when tendons are placed under two different states of static tensile load. These detectable changes between tension states are smaller than the differences that are seen between normal and pathologic tendons. Additionally, lower off-resonance saturation frequencies (3 kHz or less) are more sensitive to these changes than higher off-resonance saturation frequencies.

Acknowledgments

Contract grant sponsor: the VA Clinical Science Research and Development Service; Contract grant number: Career Development Grant 1IK2CX000749.

References

1. Benjamin M, Kaiser E, Milz S. Structure-function relationships in tendons: a review. J Anat 2008;212:211–228.
2. Sharma P, Maffulli N. Tendon injury and tendinopathy: healing and repair. J Bone Joint Surg Am 2005;87:187–202.
3. de Mos M, van El B, DeGroot J, et al. Achilles tendinosis: changes in biochemical composition and collagen turnover rate. Am J Sports Med 2007;35:1549–1556.
4. Kannus P. Structure of the tendon connective tissue. Scand J Med Sci Sports 2000;10:312–320.
5. Bydder GM. Review. The Agfa Mayneord lecture: MRI of short and ultrashort T(2) and T(2)* components of tissues, fluids and materials using clinical systems. Br J Radiol 2011;84:1067–1082.
6. Robson MD, Benjamin M, Gishen P, Bydder GM. Magnetic resonance imaging of the Achilles tendon using ultrashort TE (UTE) pulse sequences. Clin Radiol 2004;59:727–735.
7. Hodgson RJ, Grainger AJ, O'Connor PJ, et al. Imaging of the Achilles tendon in spondyloarthritis: a comparison of ultrasound and conventional, short and ultrashort echo time MRI with and without intravenous contrast. Eur Radiol 2011;21:1144–1152.
8. Syha R, Springer F, Grozinger G, et al. Short-term exercise-induced changes in hydration state of healthy achilles tendons can be visualized by effects of off-resonant radiofrequency saturation in a three-dimensional ultrashort echo time MRI sequence applied at 3 tesla. J Magn Reson Imaging 2014;40:1400–1407.
9. Hodgson RJ, Evans R, Wright P, et al. Quantitative magnetization transfer ultrashort echo time imaging of the Achilles tendon. Magn Reson Med 2011;65:1372–1376.
10. Grosse U, Syha R, Hein T, et al. Diagnostic value of T and T * relaxation times and off-resonance saturation effects in the evaluation of achilles tendinopathy by MRI at 3T. J Magn Reson Imaging 2014. doi: 10.1002/jmri.24657
11. Grosse U, Syha R, Martirosian P, et al. Ultrashort echo time MR imaging with off-resonance saturation for characterization of pathologically altered Achilles tendons at 3 T. Magn Reson Med 2013;70:184–192.
12. Fullerton GD, Rahal A. Collagen structure: the molecular source of the tendon magic angle effect. J Magn Reson Imaging 2007;25:345–361.
13. Henkelman RM, Stanisz GJ, Graham SJ. Magnetization transfer in MRI: a review. NMR Biomed 2001;14:57–64.
14. Syha R, Martirosian P, Ketelsen D, et al. Magnetization transfer in human Achilles tendon assessed by a 3D ultrashort echo time sequence: quantitative examinations in healthy volunteers at 3T. Rofo 2011;183:1043–1050.
15. Krackow KA. The Krackow suture: how, when, and why. Orthopedics 2008;31:931–933.
16. Chang EY, Du J, Bae WC, Statum S, Chung CB. Effects of achilles tendon immersion in saline and perfluorochemicals on T2 and T2*. J Magn Reson Imaging 2014;40:496–500.
17. Chang EY, Du J, Iwasaki K, et al. Single- and Bi-component T2* analysis of tendon before and during tensile loading, using UTE sequences. J Magn Reson Imaging 2014. doi: 10.1002/jmri.24758
18. Helmer KG, Nair G, Cannella M, Grigg P. Water movement in tendon in response to a repeated static tensile load using one-dimensional magnetic resonance imaging. J Biomech Eng 2006;128:733–741.
19. Monleon Pradas M, Diaz Calleja R. Nonlinear viscoelastic behaviour of the flexor tendon of the human hand. J Biomech 1990;23:773–781.
20. Pauli C, Grogan SP, Patil S, et al. Macroscopic and histopathologic analysis of human knee menisci in aging and osteoarthritis. Osteoarthritis Cartilage 2011;19:1132–1141.
21. Kannus P, Jozsa L. Histopathological changes preceding spontaneous rupture of a tendon. A controlled study of 891 patients. J Bone Joint Surg Am 1991;73:1507–1525.
22. Jarvinen M, Jozsa L, Kannus P, Jarvinen TL, Kvist M, Leadbetter W. Histopathological findings in chronic tendon disorders. Scand J Med Sci Sports 1997;7:86–95.
23. Hannafin JA, Arnoczky SP. Effect of cyclic and static tensile loading on water content and solute diffusion in canine flexor tendons: an in vitro study. J Orthop Res 1994;12:350–356.
24. Nabeshima Y, Grood ES, Sakurai A, Herman JH. Uniaxial tension inhibits tendon collagen degradation by collagenase in vitro. J Orthop Res 1996;14:123–130.
25. Stanisz GJ, Odrobina EE, Pun J, et al. T1, T2 relaxation and magnetization transfer in tissue at 3T. Magn Reson Med 2005;54:507–512.
26. Thorpe CT, Klemt C, Riley GP, Birch HL, Clegg PD, Screen HR. Helical sub-structures in energy-storing tendons provide a possible mechanism for efficient energy storage and return. Acta Biomater 2013;9:7948–7956.
27. Zhou J, Koike Y, Uhthoff HK, Trudel G. Quantitative histology and ultrastructure fail to explain weakness of immobilized rabbit Achilles' tendons. Arch Phys Med Rehabil 2007;88:1177–1184.
28. Cabral P, Paulino C, Takahashi R, Clopton P, Resnick D. Correlation of morphologic and pathologic features of the various tendon groups around the ankle: MR imaging investigation. Skeletal Radiol 2013;42:1393–1402.
29. Jozsa L, Reffy A, Kannus P, Demel S, Elek E. Pathological alterations in human tendons. Arch Orthop Trauma Surg 1990;110:15–21.